BULLETIN OF THE POLISH ACADEMY OF SCIENCES
TECHNICAL SCIENCES, Vol. 67, No. 6, 2019
DOI: 10.24425/bpasts.2019.131570

Preload monitoring in a bolted joint using Lamb wave energy

R. KĘDRA and M. RUCKA*

Department of Mechanics of Materials and Structures, Faculty of Civil and Environmental Engineering, Gdańsk University of Technology
ul. Narutowicza 11/12, 80-233 Gdańsk, Poland

Abstract. The knowledge of the load in prestressed bolted connections is essential for the proper operation and safety of engineering structures. Recently, bolted joints have become an area of intensive research associated with non-destructive diagnostics, in particular in the context of wave propagation techniques. In this paper, a novel procedure of bolt load estimation based on the energy of Lamb wave signals was proposed. Experimental tests were performed on a single lap joint of two steel plates. Ultrasonic waves were excited and registered by means of piezoelectric transducers, while precise measurement of the bolt load was obtained by means of using the force washer transducer. Experimental tests were supported by the finite element method analysis based on Schoenberg's concept. The results showed that the relationship between the bolt load and signal energy was strongly nonlinear and it depended on the location of acquisition points.

Key words: Lamb waves, steel structures, bolted joints, non-destructive testing, structural health monitoring.

1. Introduction

Bolted joints are one of the most common elements in the construction and machine industry due to their relatively low cost, durability and easy assembling process. The stiffness, load capacity and fatigue resistance of such connections can be increased by applying the controlled value of the preload during the tightening process. However, despite the simplicity of implementation, bolted joints often suffer from improper torque value, poor surface preparation or geometric deviations [1]. These assembly errors, combined with time-varying external loads [2], can lead to bolt loosening, connection failure or even entire structure collapse [3]. Therefore, to improve the safety and reliability of pre-stressed bolted connections there is a need to develop diagnostic techniques enabling continuous monitoring (e.g. [4–6]).

In recent years, intensive progress in the area of non-destructive testing of materials and structures can be observed. One of the most developed groups of techniques are those utilizing the phenomenon of elastic wave propagation, including acoustic emission, ultrasound testing, impact echo or ultrasonic-pulse velocity methods (e.g. [7–9]). Previous studies indicate that elastic waves also demonstrate great potential in assessing the condition of bolted connections. Early investigations based on ultrasonic waves for bolt loosening detection were supported by pattern recognition techniques. Mita and Fujimoto [10] developed an algorithm using the support vector machine to locate removed or loosened bolt in an aluminum connection. Park et al. [11] used both support vector machines and probabilistic neural networks for detecting the loosening of individual connectors based on the time of flight and changes of wavelet coefficients. Yang and Chang formulated [12] and experimentally verified [13] a method based on the attenuation of elastic waves to identify the location of loosened bolts in composite panels. Doyle et al. [14] observed a time delay in registered signals depending on the value of the tightening torque and analyzed the effect of the bolt state on signal energy distribution in the frequency domain. An and Sohn [15] developed a new diagnostic method using integrated impedance and elastic wave techniques and presented its potential application for the detection of bolt loosening. An integrated procedure combining guided waves and impedance signatures was proposed by Sevillano et al. [16]. They introduced a new damage indicator based on electro-mechanical power dissipation and tested its effectiveness in the detection of damage due to loose bolts. Using nonlinear acoustic phenomena, Amerini and Meo [17] introduced three indices to assess the health state of a bolted connection. The indices were based on the first-order acoustic moment, sidebands in the frequency spectrum and the second harmonic generation. Martinez et al. [18] designed and tested a phased array system, which allowed to determine the quality of a bolted connection by means of visualization of wave reflections from the contact zone. Wang et al. [19] formulated and experimentally confirmed the hypothesis about the interdependence between signal energy and bolt torque value. They tested a steel lap joint with one bolt tightened by a torque wrench and analyzed the energy of ultrasonic signals acquired in the pitch-catch mode. The obtained results revealed an approximately linear relationship between signal energy and torque up to the torque level of 70 Nm. Above this value, the saturation state was observed. Applying the real-time cross-correlation method, Ruan et al. [20] proposed a loosening indicator, which appeared to be very sensitive to even small changes of bolt torque and resistant to the noise effects. They performed experiments on a lap joint as well as on a real bolted

*e-mail: magdalena.rucka@pg.edu.pl

Manuscript submitted 2019-02-14, revised 2019-06-19, initially accepted for publication 2019-08-01, published in December 2019

structure. Tao et al. [21] examined two pieces of steel plates connected by two bolts, to which normal force was applied in a testing machine to simulate the preload. They observed that in the case of smooth contact interface, peak amplitudes of ultrasonic waves increased with the increasing bolt preload until they reached the saturation state. They also concluded that the saturation value depends strongly on surface roughness. Parvasi et al. [22] defined a tightness index based on the peak amplitude of the focused signal. They confirmed numerically and experimentally the saturation phenomenon above a certain value of the torque. Summarizing all of the works reported above, in experiments described in them, Lamb wave characteristics (such as signal energy or signal amplitude) increased with the increasing bolt load, reaching a saturation state. In addition, in most of the tests carried out, only one piezoelectric sensor working in the pitch-catch mode was used, limiting analysis of the influence of a sensor position on the Lamb wave indicators.

This study presents an approach to the condition assessment of a bolted connection using Lamb waves. Experimental investigations were performed on a single lap joint of two steel plates. In the tests conducted, Lamb wave signals were measured at several points using piezoelectric transducers and precise measurement of the bolt load was obtained by means of using the force washer transducer. The main aim of the research was the analysis of the variability of the energy of Lamb wave signals depending on the location of sensors. A novel procedure of bolt load estimation based on the energy of Lamb wave signals was proposed.

2. Experimental investigations

2.1. Description of specimens. The analysis was performed on a simple model of a single lap bolted joint. It consisted of two steel plates with the dimensions of $3\times320\times460$ mm, assembled together by one partially threaded bolt with a diameter of 12 mm, a nut (both class of 10.9) and two stainless steel washers. The lap length was set as 80 mm and the clearance hole with a diameter of 13 mm was located in the symmetry axis of the connection at a distance of 40 mm from the plate edge. The geometry of the tested connection is illustrated in Fig. 1.

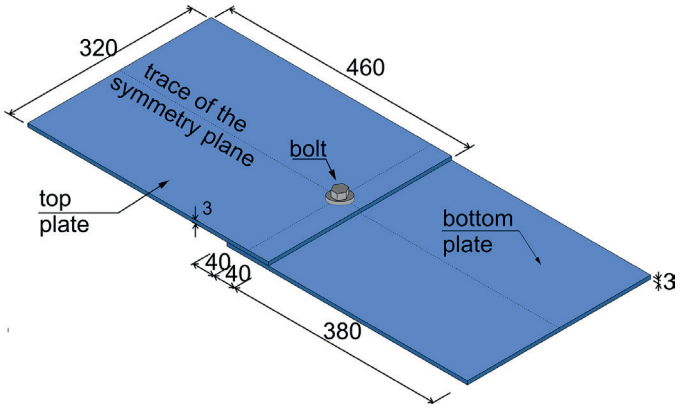

Fig. 1. Geometry of analyzed bolted lap joint (dimensions in mm)

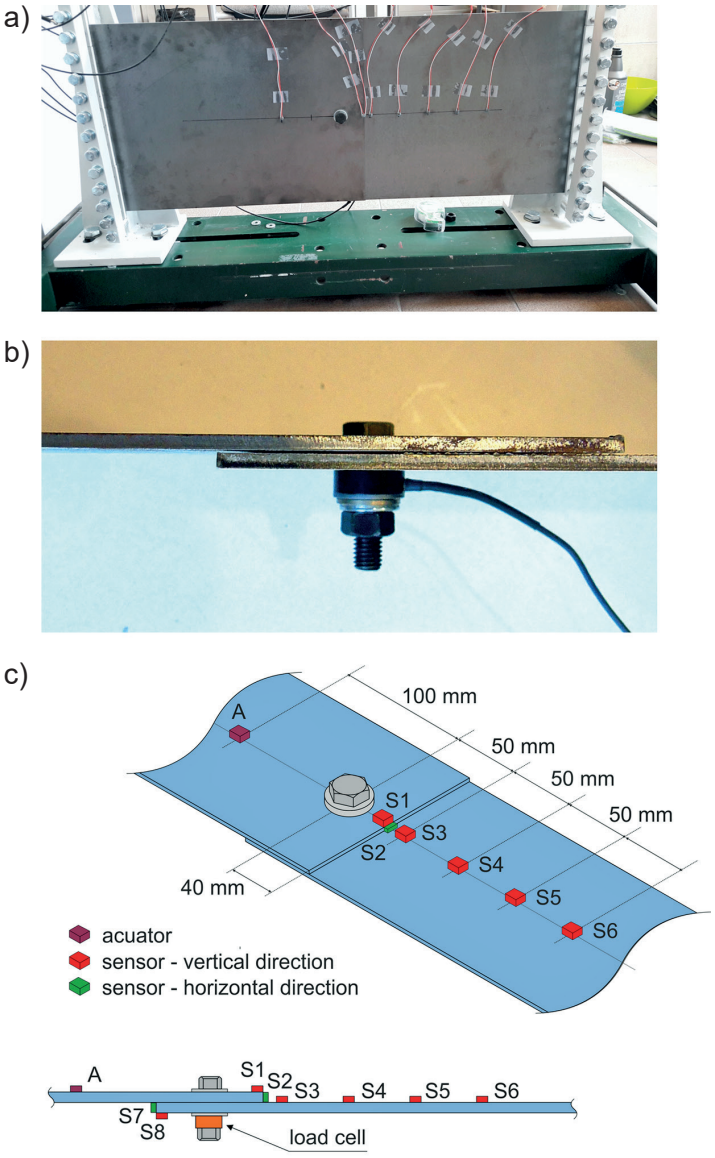

Fig. 2. Experimental set-up: (a) bolted joint mounted onto the steel frame; (b) detail showing the force sensor; (c) configuration of actuator and sensors

2.2. Experimental setup and procedure. During experimental investigations, the bolted lap joint was placed vertically in a steel frame (Fig. 2a) to minimize the influence of gravity forces on the connection area. The plates were located in parallel with each other to provide uniform pressure distribution in the radial direction during bolt pretension, which was achieved using a torque wrench. The clamp load was measured by means of the fastener force washer transducer PCB model 054212–01084 placed between the washer and nut (Fig. 2b), and force signals were registered by the LMS SCADAS data acquisition system.

Guided Lamb waves were excited and measured using the Noliac (NAC2011, NAC2024) plate piezoelectric transducers and the PAQ-16000D system. Configuration of the transducers is shown in Fig. 2c. The actuator (A) was attached to the top

plate, at a distance of 100 mm from the bolt axis. Eight sensors (S1 to S8) were located along the trace of symmetry plane of the connection. Two of them (S2 and S7) measured in-plane vibrations while the others (S1, S3 to S6 and S8) sensed out-of-plane vibrations. The excitation signal was a wave packet consisting of a 5-period sine function modulated by the Hann window with central frequency of 100 kHz.

The experiment was performed for the gradually increased value of the bolt load in the range of 0–30 kN. It was checked that the force level of 30 kN corresponded to torque of approximately 100 Nm in value. Each time after the tightening process, the bolt load was measured by the load cell and then the Lamb waves were excited and recorded. The voltage signals of 25 ms in length were measured with a sampling frequency of 2 MHz, and then they were averaged 5 times to reduce the noise influence. The experiment was repeated two times. The second measurement series was conducted after complete loosening of the bolt.

2.3. Wave propagation signals. The selected experimental results are shown in Fig. 3 as voltage signals in the time domain. In the case of sensor S1, mounted near the edge of the top plate, several different wave packets can be distinguished at the initial time period of 0.6 ms in length (Fig. 3a).

The first one is associated directly with propagation of the wave front through the contact zone along the joint axis and it is separable only by providing suitable plate width. The second one and a number of others are the effects of the reflection of the wave from the lateral edges of the plate. It can be observed that the amplitude of the first wave packet decreases significantly with the increase of the bolt load value. After reaching the contact zone, the wave is partially transmitted to the second plate. The contact area becomes the source of a new wave, which next spreads in all directions in the bottom plate. Due to the short lap length, the wave front propagating in a backward direction is almost immediately reflected in the free edge of the bottom plate. This results in wave interference and it can be observed as the first elongated wave packet in the initial part of the signal registered by sensors S3, S6 and S7 (Figs 3b–d). The effect is more visible for higher values of the bolt load. It should also be noted that amplitudes of this initial wave packets are small compared to the next wave packet and they exhibit non-linear dependence on the value of the bolt force.

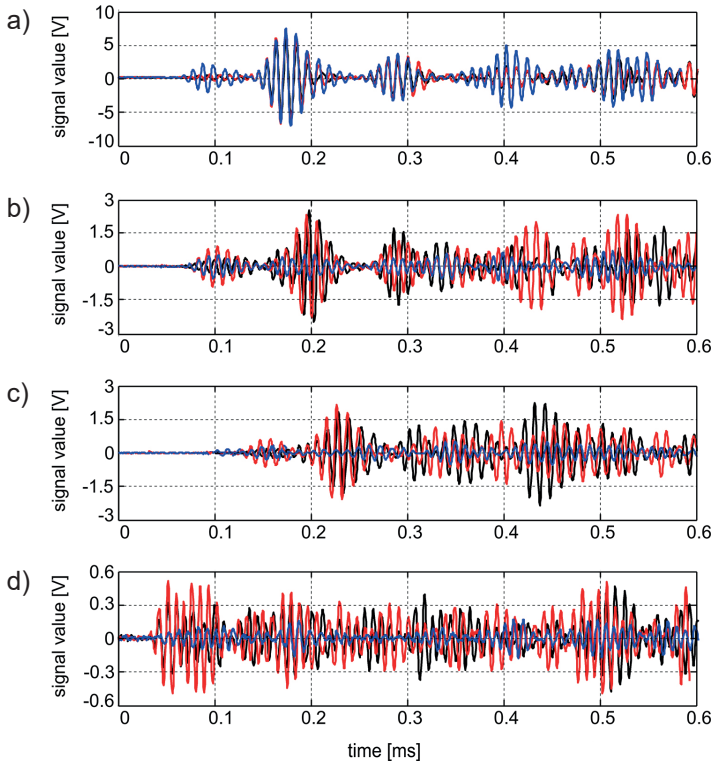

Fig. 3. Output voltage signals registered by sensor: a) S1, b) S3, c) S6 and d) S7 for different values of bolt load (blue line – bolt load of 0 kN, red line – bolt load of 0.23 kN and black line – bolt load of 2.79 kN)

3. Diagnostics using the signal energy

3.1. Formulation of the signal energy. It can be seen that despite the significant width of the investigated connection, the registered wave propagation signals contain many overlapping wave packets, which result from wave reflections from free edges of the jointed elements. This effect becomes more significant for narrower or more complex connections and it makes the qualitative comparison of signals extremely difficult. Therefore, quantitative comparison of signals constitutes a very attractive alternative. One of the simplest and most efficient indicators relies on the energy of signals. This approach is commonly used in non-destructive testing of structures in which unclear and complicated wave signals have been registered due to interaction with damage or discontinuity. The energy of a signal can be defined in both time and frequency domains. The classical definition of the total energy of a continuous time domain signal $x(t)$ can be written as [23]:

$$E = \int_{-\infty}^{\infty} [x(t)]^2 dt. \tag{1}$$

In equation (1) the energy is calculated over the interval of $<-\infty; \infty>$. In the case of experimental signals with a finite length, the energy can be determined from the following relation:

$$E = \sum_{k=n_1}^{n_2} x_k^2 \tag{2}$$

where x_k denotes the k-th value of a discrete signal and the summation is calculated within a given time interval $<n_1; n_2>$. Therefore, it must be assumed that outside the specified range, the signal has only zero or very close to zero values, so signal energy in the range is negligible. This requirement is usually easy to meet due to the decaying character of transient signals. An additional difficulty is generated by a noise contained in the signal, which can be reduced by using multiple measure-

ments and averaging or filtering procedures. The signal energy calculated according to equation (2) can be treated directly as a quantitative indicator of a loosening/tightening state and it can be intended to evaluate the damage state.

3.2. Experimental results. The results of the wave energy versus the bolt load for the investigated experimental model of the bolted lap joint are shown in Fig. 4. The values of signal energy were calculated according to equation (2) within the time interval of 0–25 ms. In general, the results for individual sensors can be divided into two groups depending on the sensor position. The decisive factor was the position of the measuring point relative to the contact surface between the plates. In the case of sensors S1 and S2, attached to the top plate, the significant drop in signal energy can be observed within the initial range of the bolt load (from 0 kN to approximately 5 kN for sensor S1 and 10 kN for sensor S2).

For sensors S3 to S8, which were situated on the opposite side of the contact surface, the trend was reversed. The relationship between the energy and the bolt load depended on the location of the sensor. In the case of sensors S3–S6, three phases can be observed. In the initial range of force (from 0 kN to approximately 10 kN), the value of signal energy increased with the increasing bolt load. Then, the energy value changed slightly in the range of 10–25 kN and finally, some slopes were visible above 25 kN. The relationship between the energy and the bolt load for sensors S7 and S8 was twofold: initially, in the range from 0 kN to approximately 10 kN, rapid growth could be observed and then the decrease of energy value occurred.

3.3. FEM analysis of wave propagation through bolted lap joint. In order to analyze trends of the energy of signals, a simplified two-dimensional, plane strain model of the lap joint was created in the Abaqus FEA software. The material was assumed as linear, elastic and isotropic with Young's modulus $E = 200$ GPa, Poisson's ratio $\nu = 0.3$ and mass density $\rho = 7850$ kg/m^3. The geometry of the numerical model is shown in Fig. 5. Excitation of the Lamb wave was achieved by the time-varying point load applied at the top surface of the first part of the model (at point A), while the registration of acceleration signals was carried out at the seven points (P1–P8) situated along the wave propagation path (analogously to experimental investigations).

The interaction between elements (Fig. 6a) was simulated based on Schoenberg's concept [24], which implies that imperfect contact conditions at boundaries can be modelled assuming the discontinuity of the displacement field. In the FEM model, it was realized introducing normal and tangential spring elements between two parts of the structure (Fig. 6c). The ratio between tangential stiffness k_t and normal stiffness k_n was set

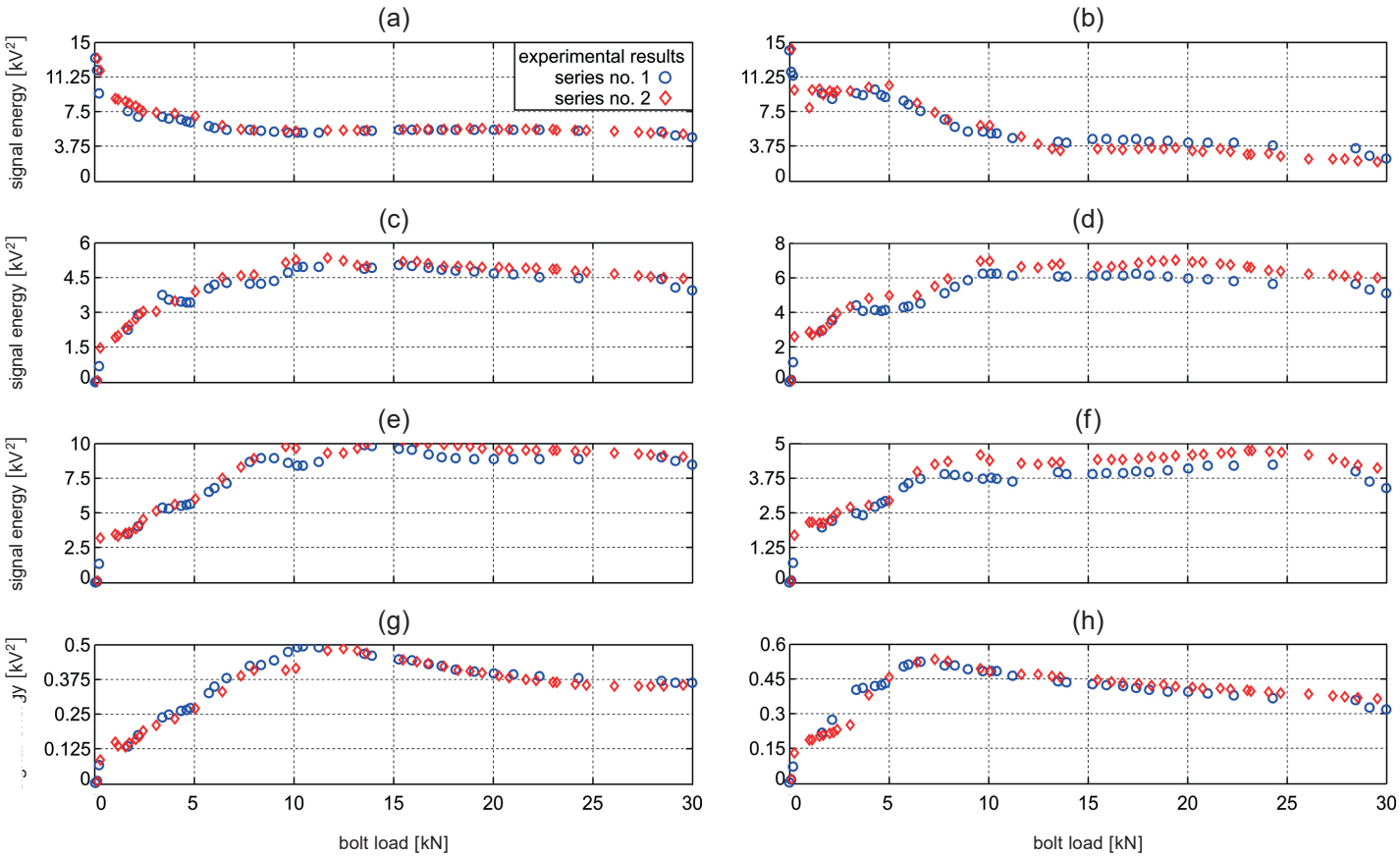

Fig. 4. Experimental relationship between the bolt load and energy of signals registered by sensors: a) S1, b) S2, c) S3, d) S4, e) S5, f) S6, g) S7, h) S8 in two measurement series

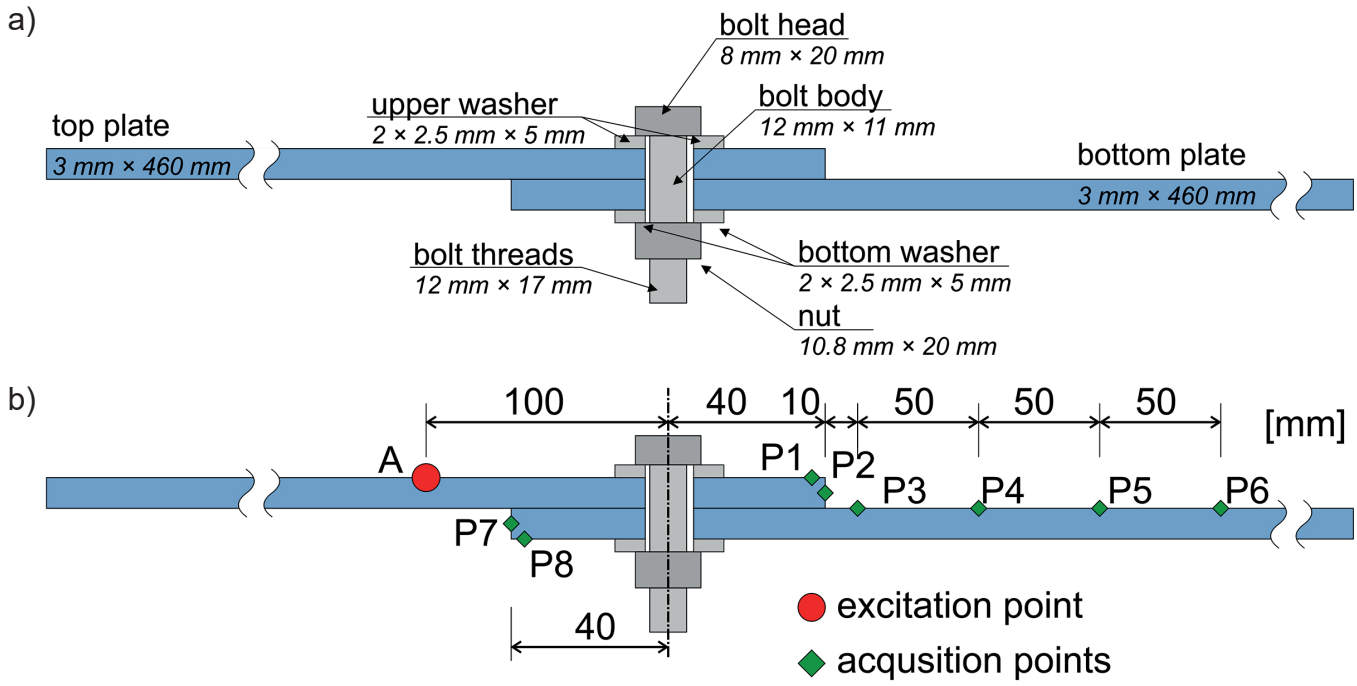

Fig. 5. Geometry of the numerical model of the lap bolted joint (a) and configuration of excitation and acquisition points (b)

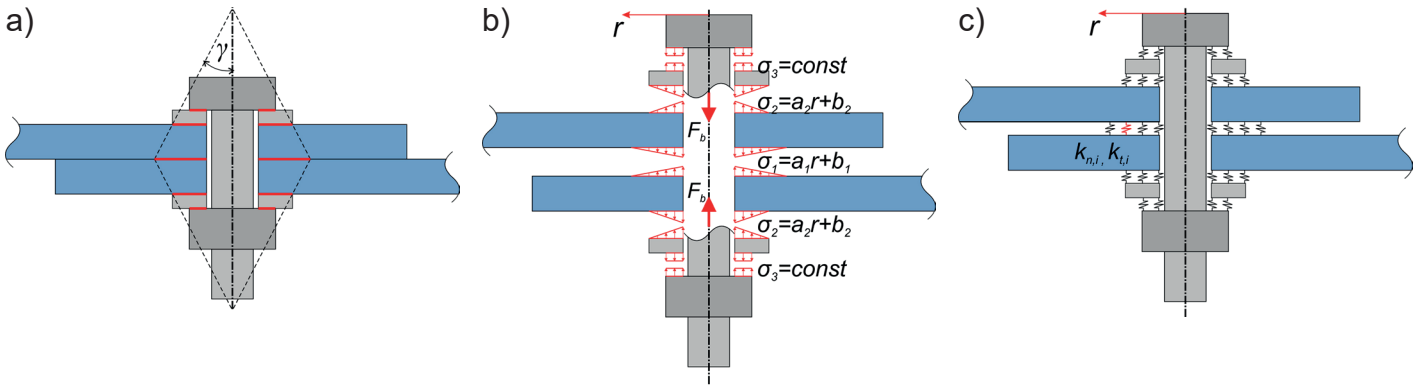

Fig. 6. Sketch of the contact region: a) range of the contact zone, b) distribution of contact stresses, c) illustration of Schoenberg's concept

as 0.8235 according to the formula determined by Mindlin [25] for the axisymmetric Hertzian contact:

$$\frac{k_t}{k_n} = \frac{2(1-\nu)}{2-\nu}. \tag{3}$$

The value of normal stiffness in the model was determined assuming that it is proportional to the average value of contact pressure in a given area:

$$k_n = \lambda \int_{\Omega} \sigma \, d\Omega = \lambda \bar{\sigma} \Omega \tag{4}$$

which is in compliance with the results of experimental research of wave propagation [26]. The value of the coefficient λ was set as $3.33 \cdot 10^7$ m^{-1}.

According to previous numerical FEM analysis [27], linear contact stress distribution was applied in the model (Fig. 6b). At the contact plate-plate interface and the plate-washer interface, triangular distribution in the radius direction was assumed with the maximum value of the contact stresses at the edge of the bolt hole. At the contact surface between the bolt head/nut and the washer, local disturbances of stress distribution were omitted and a constant stress value was assumed. The relation between stress values at particular levels has been determined assuming that the resultant of contact stresses must be equal to the bolt force. For example, for the bolt load value of 30 kN, the maximum pressure between plates was 141 MPa and zero value was assumed at the distance of 7.5 mm from the bolt axis. The pressure at plate-washer interfaces changed from 208 MPa to 0 MPa for a radial coordinate of 5.5 mm. The stresses between the bolt

head/nut and washer were constant and equal to 140 MPa along the entire contact area.

In order to simulate the spatial character of the wave propagation phenomenon, the damping model proposed by Ramadas et al. [28] was used in the FEM analysis performed. The coefficient of the mass-proportional damping matrix $\alpha = 596.8$ was calculated in terms of the assumed value of the attenuation coefficient $k = 0.2$ Np/m and the analytically determined group velocity $c_g = 2984$ m/s A_0 Lamb mode at the frequency of 100 kHz according to equation [28]:

$$\alpha = 2kc_g. \tag{5}$$

The lap joint model was discretized (see Fig. 7) based on the structural mesh using bilinear plane strain quadrilateral finite elements (CPS4) with dimensions not exceeding 0.5 mm in the direction of wave propagation. Furthermore, the mesh has been additionally refined to the size of 0.1×0.2 mm at the area of the location of springs. The free boundary conditions were established at all edges. The time step of numerical implicit integration was assumed as 50 ns.

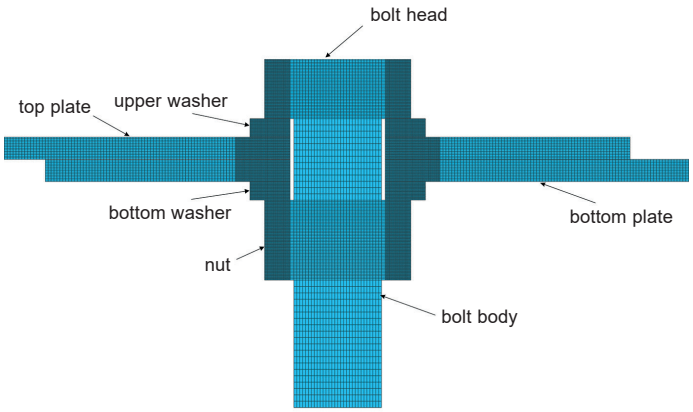

Fig. 7. Finite element mesh in a lap region of the numerical model

The relationships between the energy of numerical signals registered in points P3–P8 and the bolt load are presented in Fig. 8. The results for points P1 and P2 were omitted in further analysis, due to the inability of the 2D numerical model to simulate wave propagation in the connection area in an exact manner. In the experimental model, the propagating disturbance was transmitted along the edge of the bolt hole, while in the numerical model for small value of contact stiffness, the wave did not reach those points.

In all analyzed points (P3–P8), the increase in the energy value was observed with increasing contact stiffness. The results of the FEM analysis confirmed that the relationship between these two parameters is strongly nonlinear. The largest increase in the signal energy value was observed for the initial bolt load range (below 0.1 kN). In the case of experimental tests, it ranged from 25% (sensors S7, S8) to 50% (in the case of sensors S3–S6) of the maximum registered energy value. In numerical analyses, this initial increase was even larger, and the energy for individual sensors reached 60–75% of the maximum value. This effect occurred in the FEM results because of not taking account of energy dissipation in the contact zone and assuming a strictly linear relationship between contact pressure and stiffness; however, it did not affect the correctness of the numerical analysis conducted. Results of FEM analysis also confirmed that the position of the sensor affected the signal energy variability. In the case of points located near the contact zone (P7, P8), it was possible to observe a local extreme of the signal energy in the initial bolt load range. This was related

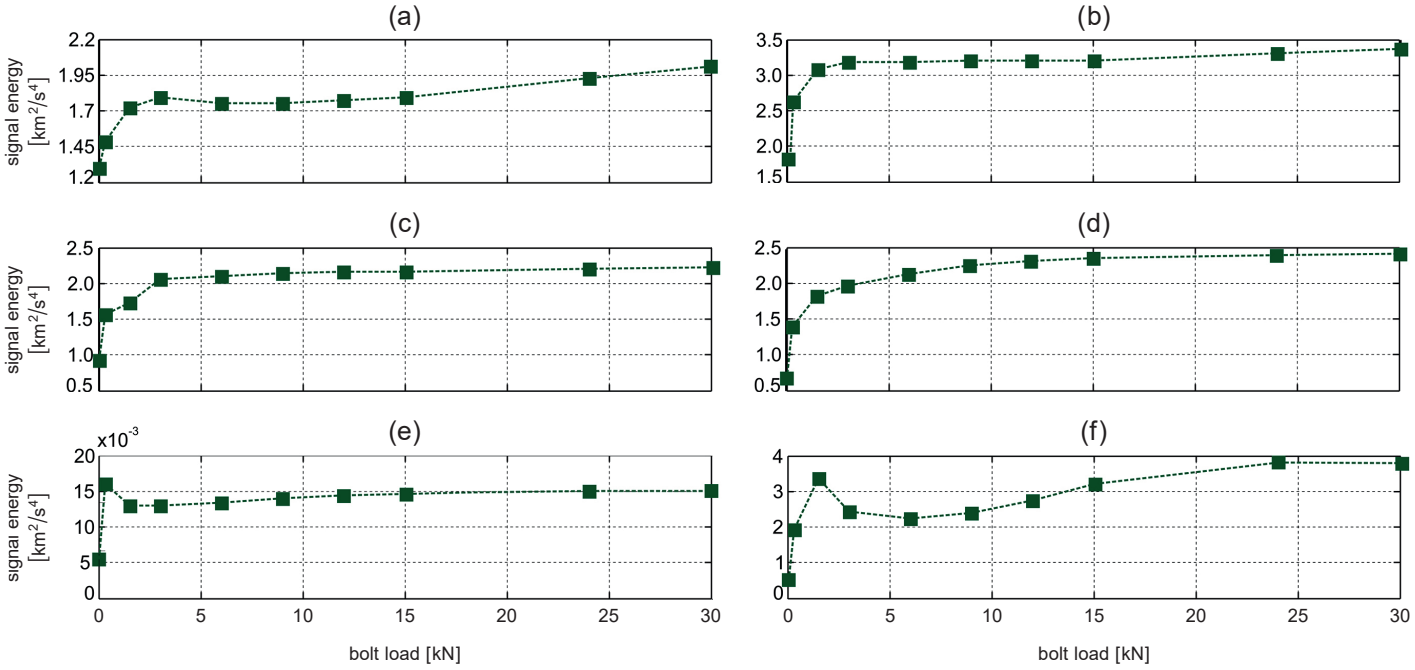

Fig. 8. Numerical relationship between the bolt load and energy of signals calculated in points: a) P3, b) P4, c) P5, d) P6 e) P7 and f) P8

to multiple reflections of propagating disturbances from the plate edges and contact surface (interfering waves disturbed the trend in energy variation). It should be noted that in the case of experimental research, this effect has not been visible, which indicated a high impact of reflections from the longitudinal edges of plates in a three-dimensional joint on the value of signal energy. At the points located at a larger distance from the contact zone, the signal energy became more monotonic. In the case of point P3, only the local extremum of the energy for approximately 3kN can be observed. In points P4, P5 and P6, the relationship became strictly growing, and as distance from the contact zone increased, the extreme value of energy was achieved for the smaller value of the bolt load.

3.4. Procedure of bolt load estimation based on signal energy. In this section, a procedure for the estimation of bolt preloading is proposed. From the numerical results (Fig. 8a–d), it is visible that for all sensors located at the bottom plate, the relationship between the bolt load and signal energy can be approximated by an exponential function until the energy reaches the extreme value E_{max} corresponding to the saturation state. Therefore, only two points represented by bolt load values (F_{b1} and F_{b2}) and two energy values (E_1 and E_2) corresponding to them are required to determine the function formula. Based on those parameters and the actual value of the signal energy E, the current value of the bolt load F_b can be calculated from the following equation:

$$F_b = e^{\frac{E}{E_2 - E_1}\left[\ln(F_{b2}) - \ln(F_{b1}) - E_1\ln(F_{b2}) + E_2\ln(F_{b1})\right]}. \tag{6}$$

Determination of the saturation state is crucial for the correctness of the approximation. The results presented in Fig. 4 indicated that in the case of experimental results the saturation state was achieved below 10 kN and its appearance depended on the sensor location. In the case of sensor S6 (Fig. 4f), the saturation level was observed for the bolt load equal to 8.33 kN and this value was adopted in further considerations as the upper limit of energy growth.

Figure 9 shows the exemplary results of estimation of the bolt load based on the experimental data obtained for sensors S3–S6 in the measurement series No. 1. The same pair of points was chosen for all sensors to determine the course of the energy versus bolt load dependence. The first point of approximation was chosen as the point for which the bolt load value exceeded 1 kN, while the second point was established as an upper limit of the analyzed range. Additionally, the results of experimental data fitting the exponential function using the least squares method (LSM) were plotted in Fig. 9.

It can be seen that the value of the bolt load estimated using the proposed methodology corresponded well with the real preload value for senor S6. This was confirmed by the high value of the coefficient of determination $R^2 = 0.922$. For other sensors (S3–S5), it had slightly lower values of approximately 0.82. However, it should be noted that with the increase of

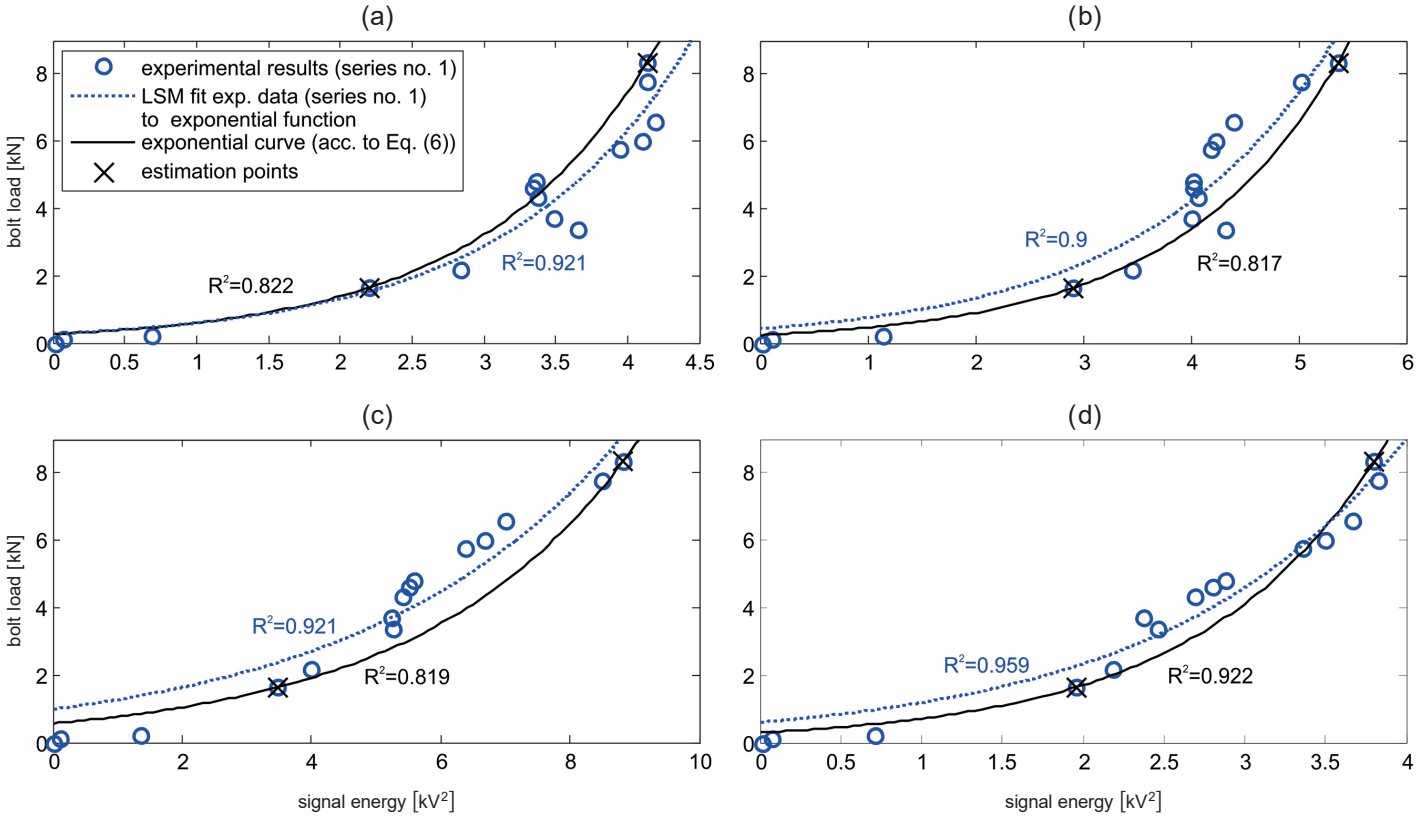

Fig. 9. Exemplary results of bolt load estimation using the proposed approach based on experimental signals (series No. 1) registered by sensor: a) S3, b) S4, c) S5 and d) S6

the distance from the contact zone the maximum difference between the measured and estimated force value decreased. It amounted, respectively, to: 2.180 kN for sensor S3, 2.202 kN for sensor S4, 1.797 kN for sensor S5, and 1.32 for sensor S6. The values of coefficients of determination obtained by the LSM were slightly higher and they ranged from 0.9 for sensor S4 to 0.959 for sensor S6. In general, the bolt load values determined for selected points were lower than the corresponding values obtained using the LSM.

4. Conclusions

The work presented the analysis of elastic wave propagation in the single lap bolted joint. Experimental tests were supported by FEM analysis based on Schoenberg's concept. The research focused on the changes of the quantitative parameter in the form of the energy of recorded Lamb wave signals.

In the research, one actuator and eight sensors were used. It has been shown that the relationship between the bolt load and signal energy was strongly nonlinear and it depended on the location of acquisition points. The main influence on the character of variability (increasing or decreasing) came from the position of the sensor relative to the contact region. Both experimental and numerical results confirmed that as the distance from the contact zone increased, the relationship between the energy value and the bolt load became monotonic increasing.

The novel procedure of bolt load estimation based on the energy of Lamb wave signals was proposed. It has been revealed that for sensors located at a suitable distance from the contact zone, the relationship between the bolt load and signal energy can be approximated by means of an exponential function based on two calibration measurements. The procedure was successfully applied in the monitoring of the preload of the tested bolted lap joint.

Future studies will aim at verifying the reliability of the proposed procedure on the example of joints with different geometries. Moreover, the influence of various material parameters and surface roughness could also be investigated.

Acknowledgements. The research work was carried out within project No. 2015/19/B/ST8/00779, financed by the National Science Centre, Poland. Abaqus calculations were carried out at the Academic Computer Centre in Gdansk. The support is greatly acknowledged by the authors.

References

[1] D. Chen, Y. Ma, B. Hou, R. Liu, and W. Zhang, "Tightening Behavior of Bolted Joint with Non-parallel Bearing Surface", *Int. J. Mech. Sci.*, 153–154, 240–253 (2019).

[2] J. Seo, J. Hu and K.-H. Kim, "Analytical Investigation of the Cyclic Behavior of Smart Recentering T-Stub Components with Superelastic SMA Bolts", *Metals*, 7, 386, (2017).

[3] J. Álvarez, R. Lacalle, B. Arroyo, S. Cicero, and F. Gutiérrez-Solana, "Failure Analysis of High Strength Galvanized Bolts Used in Steel Towers", *Metals*, 6, 163, (2016).

[4] H. Cho and C.J. Lissenden, "Structural health monitoring of fatigue crack growth in plate structures with ultrasonic guided waves", *Struct. Heal. Monit.* 11, 393–404 (2012).

[5] B. Yang, F.-Z. Xuan, Y. Xiang, D. Li, W. Zhu, X. Tang, J. Xu, K. Yang, and C. Luo, "Lamb Wave-Based Structural Health Monitoring on Composite Bolted Joints under Tensile Load", *Materials*, 10, 652, (2017).

[6] M. Rucka, "Monitoring Steel Bolted Joints during a Monotonic Tensile Test Using Linear and Nonlinear Lamb Wave Methods: A Feasibility Study", *Metals*, 8, 683, (2018).

[7] J. Hoła, J. Bień, L. Sadowski, and K. Schabowicz, "Non-destructive and semi-destructive diagnostics of concrete structures in assessment of their durability, *Bull. Pol. Ac.: Tech.* 63, 87–96, (2015).

[8] A. Garbacz, "Application of stress based NDT methods for concrete repair bond quality control", *Bull. Pol. Ac.: Tech*. 63, 77–85, (2015).

[9] B. Goszczyńska, G. Świt, and W. Trąmpczyński, "Analysis of the microcracking process with the Acoustic Emission method with respect to the service life of reinforced concrete structures with the example of the RC beams", *Bull. Pol. Ac.: Tech.* 63, 55–63, (2015).

[10] A. Mita and A. Fujimoto, "Active detection of loosened bolts using ultrasonic waves and support vector machines", in: *Proceeding 5th Int. Work. Struct. Heal. Monit.*, pp. 1017–1024, 2005.

[11] S.-H. Park, C.-B. Yun, and Y. Roh, "PZT-induced Lamb Waves and Pattern Recognitions for On-line Health Monitoring of Jointed Steel Plates", in: *Proc. SPIE 5765, Smart Struct. Mater. 2005 Sensors Smart Struct. Technol. Civil, Mech. Aerosp. Syst.*, pp. 364–375, 2005.

[12] J. Yang and F.K. Chang, "Detection of bolt loosening in C-C composite thermal protection panels: I. Diagnostic principle", *Smart Mater. Struct.* 15, 581–590, (2006).

[13] J. Yang and F.K. Chang, "Detection of bolt loosening in C-C composite thermal protection panels: II. Experimental verification", *Smart Mater. Struct.* 15, 591–599, (2006).

[14] D. Doyle, A. Zagrai, B. Arritt and H. Çakan, "Damage detection in bolted space structures", *J. Intell. Mater. Syst. Struct*. 21, 251–264, (2010).

[15] Y.K. An and H. Sohn, "Integrated impedance and guided wave based damage detection", *Mech. Syst. Signal Process*. 28, 50–62, (2012).

[16] E. Sevillano, R. Su and R. Perera, "Damage detection based on power dissipation measured with PZT sensors through the combination of electro-mechanical impedances and guided waves", *Sensors*, 16, 639, (2016).

[17] F. Amerini and M. Meo, "Structural health monitoring of bolted joints using linear and nonlinear acoustic/ultrasound methods", *Struct. Heal. Monit.* 10, 659–672, (2011).

[18] J. Martinez, A. Sisman, O. Onen, D. Velasquez, and R. Guldiken, "A synthetic phased array surface acoustic wave sensor for quantifying bolt tension", *Sensors*, 12, 12265–12278, (2012).

[19] T. Wang, G. Song, Z. Wang, and Y. Li, "Proof-of-concept study of monitoring bolt connection status using a piezoelectric based active sensing method", *Smart Mater. Struct*. 22, 087001, (2013).

[20] J. Ruan, Z. Zhang, T. Wang, Y. Li, and G. Song, "An anti-noise real-time cross-correlation method for bolted joint monitoring using piezoceramic transducers", *Smart Struct. Syst*. 16, 281–294, (2015).

[21] W. Tao, L. Shaopeng, S. Junhua, and L. Yourong, "Health monitoring of bolted joints using the time reversal method and piezoelectric transducers", *Smart Mater. Struct.* 25, 25010, (2016).

[22] S.M. Parvasi, S.C.M. Ho, Q. Kong, R. Mousavi, and G. Song, "Real time bolt preload monitoring using piezoceramic transducers and time reversal technique – A numerical study with experimental verification", *Smart Mater. Struct*. 25, 1–11, (2016).
[23] M. Mandal and A. Asif, *Continuous and Discrete Time Signals and Systems*, Cambridge University Press, 2007.
[24] M. Schoenberg, "Elastic wave behavior across linear slip interfaces", *J. Acoust. Soc. Am*. 68, 1516–1521, (1980).
[25] R.D. Mindlin, "Compliance of elastic bodies in contact", *J. Appl. Mech*. 16, 259–268, (1949).
[26] S. Biwa, S. Hiraiwa, and E. Matsumoto, "Stiffness evaluation of contacting surfaces by bulk and interface waves", *Ultrasonics* 47 123–129 (2007).
[27] R. Kędra and M. Rucka, "Modelling of elastic wave propagation in a bolted joint using a thin layer of shell elements", in: *Shell Struct. Theory Appl*. 4, CRC Press/Balkema, pp. 293–296, 2018.
[28] C. Ramadas, K. Balasubramaniam, A. Hood, M. Joshi, and C.V. Krishnamurthy, "Modelling of attenuation of lamb waves using rayleigh damping: Numerical and experimental studies", *Compos. Struct*. 93, 2020–2025 (2011).